









Determination of the solar fraction for optimized parabolic concentrator solar collector networks

Determinación de la fracción solar para redes termosolares optimizadas conformadas por la tecnología de colectores tipo canal parabólico

Lizárraga-Morazán, Juan Ramón <sup>a</sup> & Picón-Núñez, Martín <sup>\*b</sup>.

<sup>a</sup>  Universidad de Guanajuato •  KXB-6991-2024 •  0000-0002-7733-5621 •  83138

<sup>b</sup>  Universidad de Guanajuato •  AHA-5481-2022 •  0000-0002-0793-192X •  12408

CONAHCYT classification:

Area: Engineering  
Field: Engineering  
Discipline: Energy engineering  
Subdiscipline: Solar energy

 <https://doi.org/10.35429/EJDRC.2024.10.18.1.9>

History of the article:

Received: October 12, 2024

Accepted: December 10, 2024

\*  [picon@ugto.mx](mailto:picon@ugto.mx)

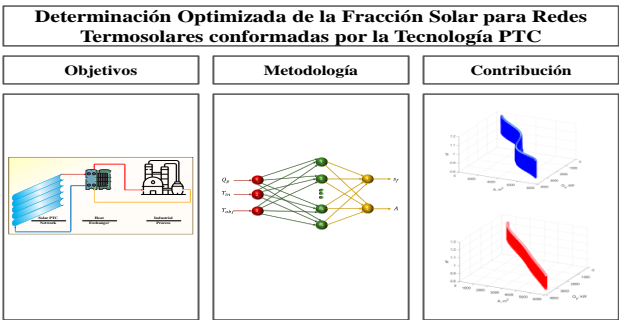
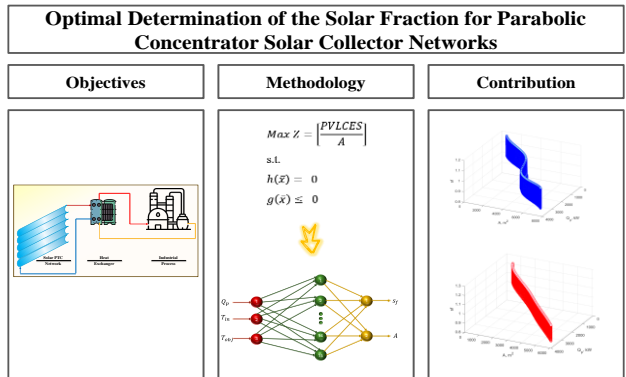


Abstract

Studies show that the solar fraction of most solar thermal plants that supply heat to industrial processes ranges from 5-60%. The main limiting factor for increasing this value to 100% is the installation area. This work presents a study of the solar fraction parameter in optimized designs of systems using parabolic trough collector technology. An optimization process using Mixed-Integer Nonlinear Programming with 9 decision variables is proposed, employing the heuristic technique of Particle Swarm Optimization coupled with a transient thermohydraulic-economic model. The inlet temperature of the heat transfer fluid was varied from low to high, as well as the temperature and load required by the industrial process to obtain networks with optimized area, structure, and operating conditions. For predicting the solar fraction parameter and optimized network area, a regression using artificial neural networks was performed. It was found that it is possible to obtain flexible optimized networks capable of operating with average sf values of 1.05 throughout the year, and with a minimum area that supports changes in the operating conditions of temperature and thermal load of the process in the range of 70-400°C and 0.4-4 MW, respectively.

Resumen

Estudios muestran que la fracción solar de la mayoría de las plantas termosolares que suministran calor a procesos industriales rondan en el rango de 5-60 %; siendo el principal factor limitante para incrementar este valor al 100% el área de instalación. Este trabajo presenta un estudio del parámetro de fracción solar en diseños optimizados de sistemas que emplean la tecnología de colector tipo tiro parabólico. Se propone un proceso de optimización tipo mixto entero no lineal con 9 variables de decisión, empleando la técnica heurística tipo Particle Swarm Optimization acoplada a un modelo termohidráulico-económico transiente. Se varió la temperatura de entrada del fluido de trabajo en el rango bajo a alto; al igual que la temperatura y carga requeridas por el proceso industrial para obtener redes con área, estructura y condiciones operativas optimizadas. Para la predicción del parámetro de fracción solar y área de la red optimizadas, se realizó una regresión empleando redes neuronales artificiales. Se encontró que es posible obtener redes optimizadas flexibles, capaces de operar con valores sf promedio de 1.05 a lo largo del año; y con área mínima que soporta cambios en las condiciones de operación de temperatura y carga térmica del proceso en el rango de 70-400 °C, y 0.4-4 MW, respectivamente.



Solar, Fraction, Optimization, Heat, Industrial, Processes

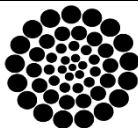
Solar, Fracción, Optimización, Energía, Industriales, Procesos

**Citation:** Lizárraga-Morazán, Juan Ramón & Picón-Núñez, Martín. [2024]. Determination of the solar fraction for optimized parabolic concentrator solar collector networks. ECORFAN-Journal Democratic Republic of Congo. 10[18]1-9: e41018109.



ISSN 2414-4924 /© 2009 The Author[s]. Published by ECORFAN-Mexico, S.C. for its Holding Democratic Republic of Congo on behalf of ECORFAN-Journal Democratic Republic of Congo. This is an open access article under the CC BY-NC-ND license [<http://creativecommons.org/licenses/by-nc-nd/4.0/>]

Peer Review under the responsibility of the Scientific Committee **MARVID®**- in contribution to the scientific, technological and innovation Peer Review Process by training Human Resources for the continuity in the Critical Analysis of International Research.



**RENIECYT**  
Registro Nacional de Instituciones y  
Empresas Científicas y Tecnológicas

**1702902 CONAHCYT**

## Introduction

Inevitably, economic development goes hand in hand with industrial growth. The industrial sector consumes 32-35% of the world's total energy (IRENA, 2024). Climate change has driven the creation of projects to facilitate the energy transition. The United Nations' 2030 Agenda sets goal number 7 as the use of affordable and clean energy (United Nations Sustainable Development GOALS, 2024). Recently, the UAE COP28 (United Arab Emirates - United Nations Climate Change Conference) issued an urgent call to triple renewable energy and double energy efficiency by 2030 to reduce CO<sub>2</sub> emissions into the atmosphere (UAE Consensus, 2024).

The economic recovery following the Covid-19 pandemic and the response to the global energy crisis have boosted investment in clean energy, reaching a record \$1.7 trillion USD in the first half of 2023, compared to just \$0.9 trillion USD in fossil energy investment (Birol, 2023). Solar energy is a clean and unlimited alternative that can be harnessed in various ways.

One of these is through the replacement of conventional industrial thermal processes with solar thermal networks known as Solar Heat for Industrial Processes (SHIP), (Figure 1).

In 2012, there were 25 SHIP solar thermal networks installed worldwide. By the end of 2019, this number had increased to 817, representing an increase of 187 MW. The most used technology for these systems is the Parabolic Trough Collector (PTC) (Epp & Krüger, 2017).

By 2022, 90% of SHIP networks employed PTC technology (Adib & Zervos, 2023).

As of the end of March 2023, the total installed area with PTC equipment reached 680,000 m<sup>2</sup> across 366 systems (AEE INTEC, 2024). PTC technology is characterized by its ability to achieve temperature ranges from 50°C to 400°C (Kalogirou, 2019).

## Box 1

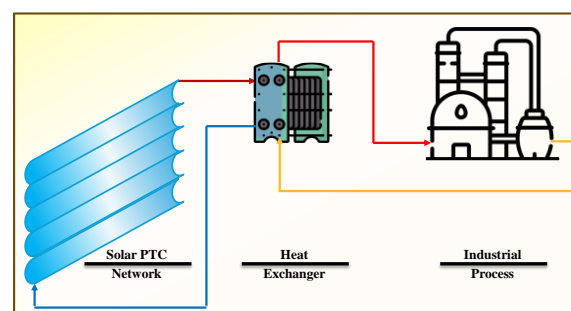


**Figure 1**

SHIP layout.

*Source: Own elaboration*

On the other hand, the solar fraction, which is the focus of this research, is an indicator used to evaluate the performance of solar thermal systems.

It compares the clean energy harvested to the energy required by the process. Despite its importance, there are few recent studies on this indicator as indicated by the following literature review.

Vanoni et al., 2006 analysed solar thermal networks in Greece, Wallonia, and Germany, focusing on industrial sectors such as chemicals, food, tobacco, textiles, and leather, among others.

They determined that a 30% solar fraction of the total energy demand of these processes is achieved. Mueller et al., 2004 conducted a technical study of solar heating plants in Austria, considering low (100°C) and medium (250°C) temperature levels, and determined an overall solar fraction of 16% of the sector's total demand.

Van de Pol & Wattimena, 2001 estimated a 30% solar fraction of the final energy demand for heating purposes in the dutch industry. They stated that the available area is the greatest limitation of solar thermal systems. Lauterbach et al., 2012 determined an overall solar fraction of 18% in the industrial sector of Germany.

The company Aiguasol analysed the Chilean industry within the APPSOL project, considering an overall solar fraction of 30% (González-García, 2018). Jia et al., 2018 found that the solar fraction in thermal industrial processes in China ranges from 5% to 10%.

In the study reported by Schweiger et al., 2000, the potential of industrial solar thermal networks in Spain and Portugal was analysed, finding a solar fraction range with minimum and maximum values of 6% to 60%.

The researchers also concluded that the available area is the limiting factor in most cases. Aste et al., 2012 determined the optimal solar fraction of hybrid collector systems (PVT - Photovoltaic-Thermal), using an economic and energy analysis with the TRNSYS platform for the cities of Rome, Palermo, and Milan (Italy

They concluded that the optimal solar fraction for these systems is 40-60%, which is lower than the recommended 70% for conventional solar thermal systems. Reiter et al., 2016 conducted a feasibility study to determine the appropriate area for the solar thermal network and thermal storage system of a district heating located in Graz, Austria, using dynamic simulation, as well as an economic and legal analysis.

They concluded that the suitable solar fraction is 9-26%, which can be achieved with an area of 150-165 thousand square meters. Pag et al., 2022 conducted a study in Germany to determine the available area using OpenStreetMap data (OSM), which is an open collaboration database project used in various educational, research, governmental, and industrial applications.

The researchers found that the available area is a limitation in 30-50% of the companies investigated. According to this study, the solar fraction in industrial SHIP systems ranges from 5-20%.

Based on the scarce information available in the open literature, the solar fraction range of installed SHIP-type solar thermal networks is between 5% and 60%, with the main limitation being the available area.

However, some questions arise: if the installation area was not a limitation, would it be preferable to aim for a solar fraction close to one in the design of a solar thermal system of these characteristics?

What is the relationship between the solar fraction and the design point at which total operating and investment costs are minimized?

This work answers these questions and presents an analysis of the behaviour of the solar fraction for different optimized design conditions for the summer and winter seasons in the city of Guanajuato, Gto., Mexico, varying the inlet temperature of the heat transfer fluid (HTF) in the low and medium ranges, as well as the temperature and thermal load required by the process in typical operating ranges.

The analysis employs a transient thermohydraulic-economic model coupled with the heuristic optimization methodology PSO (particle swarm optimization) for the design of equipment, network structure, and operating conditions that maximize thermal and economic benefits, ensuring the minimum available installed area.

Methodology

The thermohydraulic-economic model used in this research was presented and validated in the work of Lizárraga-Morazán & Picón-Núñez, 2024. The methodology includes a one-dimensional transient model for the thermohydraulic solution coupled with the economic analysis model of Present Value of Life Cycle Energy Savings (PVLCES). The methodology reported by Caballero et al., 2022 was used to determine the Life Cycle Energy Savings. The MINLP (Mixed-Integer Nonlinear Optimization) problem is presented below:

$$Max Z = \left[ \frac{PVLCES}{A} \right]$$

s.t.

$$h(\bar{x}) = 0$$
$$g(\bar{x}) \leq 0$$

[1]

Where A is the thermosolar network area. The objective function includes the two most important design parameters: the economic function that must be maximised represented by the PVLCES, and the surface area which must be minimised.

Therefore, the ratio of these two parameters is sufficient to ensure optimal design.  $h(\bar{x})$  represents the set of equations that make up the extended thermohydraulic-economic model for the solar thermal network, while  $g(\bar{x})$  represents the set of constraints imposed on the system, given by the following expressions:

$$\begin{aligned} T_o^{max} &\leq T_{HTF}^{lim} \\ PVLCEs &\geq 0 \end{aligned} \tag{2}$$

Where  $T_o^{max}$  is the maximum instantaneous useful outlet temperature generated by the solar thermal network during daily operation (9 AM – 6 PM);  $T_{HTF}^{lim}$  is the operating limit temperature of the heat transfer fluid (HTF), and  $sf$  is the solar fraction defined by the following expression:

$$sf = \frac{Q}{Q_p} \tag{3}$$

Where  $Q_p$  is the thermal load required by the process.  $Q$  is the total useful integrated heat, representing the total energy harvested by the network at the outlet temperature level required by the industrial process ( $T_{obj}$ ).

This value results from the integration of the instantaneous useful energy gained by the heat transfer fluid (HTF) during the operation time.

$$Q = \int_{t=9\ h}^{t=18\ h} q_t dt \tag{4}$$

In the optimization problem, nine decision variables were considered, including the dimensions that define the geometry of the PTC: length  $L_c$ , aperture width  $W_{aper}$ , receiver diameter  $D_i$ , glass envelope diameter  $D_{gi}$ , and PTC focal length  $f$ .

Additionally, it includes variables that define the size and structure of the network: number of collectors per line  $N_{cl}$  and total number of network lines  $N_L$ .

Finally, the model also optimizes the mass flow rate of the HTF to the network  $\dot{m}_f$  and the type of HTF. Four widely used commercial fluids were considered in the analysis: pressurized water, Syltherm-800, Therminol VP-1, and Dowtherm-A.

To solve the optimization problem, the stochastic Particle Swarm Optimization (PSO) methodology was employed.

In this technique, potential solutions are identified as particles with memory, allowing them to recognize the best solution within the feasible search space (Sharma et al., 2012), (Afzal et al., 2023).

The optimization problem was solved by varying the thermal load required by the process  $Q_p$ , the inlet temperature of the heat transfer fluid  $T_{in}$ , and the temperature required by the process ( $T_{obj}$ ) over wide intervals for typical winter and summer days. These ranges are presented in Table 1.

**Box 2**  
**Table 1**  
Independent Variable Range

$Q_p$ (kW)	400 - 4,000
$T_{obj}$ (°C)	70 - 400
$T_{in}$ (°C)	$(0.7 - 0.9) \cdot T_{obj}$

Source: Own elaboration.

Table 2 presents the parameter search space. The limits of the selected decision variables are taken from commercial equipment reported in open literature (Afzal et al., 2023).

**Box 3**  
**Table 2**  
Parameter search space

$L_c$ (m)	2-15
$W_{aper}$ (m)	0.5-9.3
$D_i$ (m)	0.01-0.08
$D_{gi}$ (m)	0.1-0.2
$f$ (m)	0.2-3
$N_{cl}$	1-40
$N_L$	1-200
$\dot{m}_f$ (kg·s <sup>-1</sup> )	0.1-10
HTF	Syltherm-800, Dowtherm-A, Therminol, VP-1, Pressurized water

Source: Own elaboration.



To have a representative sample of the ranges of the independent variables, specific values for  $Q_p$ ,  $T_{in}$  and  $T_{obj}$  were selected to cover the defined intervals. The process thermal load was divided into four levels: 400, 1,600, 2,800, and 4,000 kW.

The target temperature was divided into seven levels: 70, 125, 180, 235, 290, 345, and 400 °C; and the inlet temperature was divided into three levels: 0.7, 0.8, and 0.9  $\cdot T_{obj}$ .

The optimization problem was solved for each of the 84 combinations of  $Q_p$ ,  $T_{in}$  and  $T_{obj}$ ; and for each season. Instantaneous daily environmental data on irradiance, ambient temperature, and wind speed collected in the city of Guanajuato (21.0190° N, 101.2574° W) at the facilities of the University of Guanajuato, Mexico, were used.

The results obtained regarding the geometry of the PTC equipment that makes up the network, the size and structure of the network, and the optimized operating conditions are reported in the work of [XIX].

Finally, the solar fraction performance parameter was determined for each combination of winter and summer samples, and the regression process was carried out using classical multivariable polynomial regression techniques and neural networks.

In this work, neural network regression was successfully used to predict the solar factor and network area, as conventional regression did not yield reliable statistical results.

The multilayer perceptron (MLP), also known as a feed-forward neural network (FFNN), was the model selected for this work.

Typically, the use of MLP in regression problems requires only one hidden layer, in addition to the input and output layers.

The Levenberg-Marquardt (LM) algorithm was used in the optimization, and the sigmoid transfer function was employed in the hidden layer for signal translation between the layers of the MLP network.

Figure 2 illustrates the structure of the MLP model used in the regression for predicting the solar fraction and the area of the solar thermal network.

#### Box 4

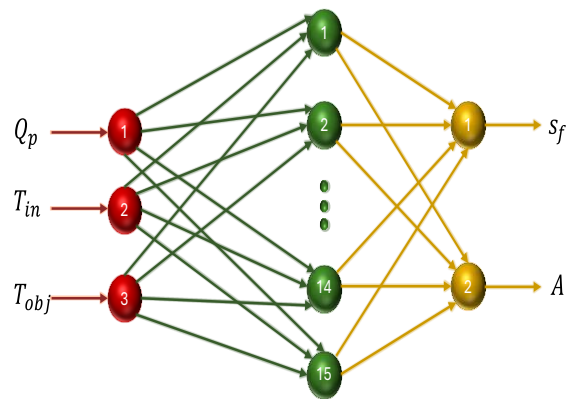


**Figure 2**

Structure of the MLP used on A - sf regression

Source: Own elaboration

#### Results

Figure 3 presents the profile of the solar fraction concerning the solar thermal area and the thermal load required by the process.

The set of points in a single colour represent the different combinations of inlet temperature and the temperature required by the process for the same heat load.

It is interesting to note that the proposed optimization process can generate flexible solar thermal networks, where the installed area allows operation over a wide range of operating conditions for  $Q_p$ ,  $T_{in}$  and  $T_{obj}$ ; while maintaining high solar fraction values.

Table 3 summarizes the most relevant statistical data of the optimized solar fraction for the winter and summer samples.

Box 5

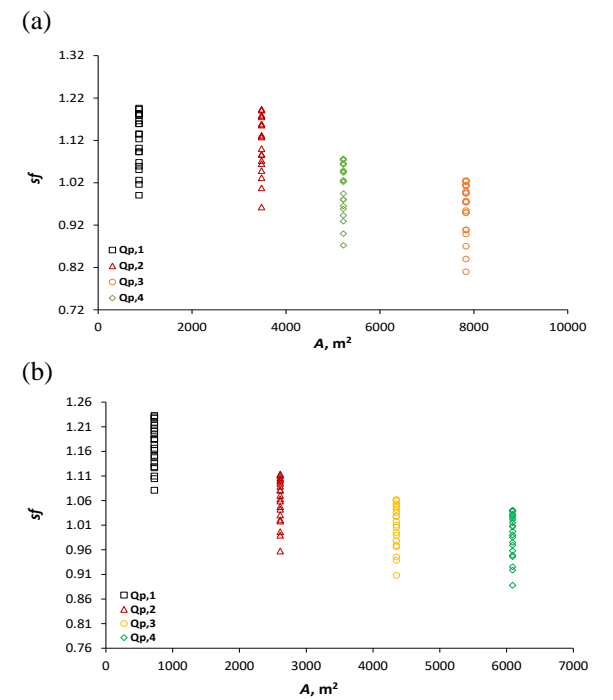


Figure 3  
sf – A profile: (a) winter and (b) summer  
Source: Own elaboration

Box 6

Table 3

sf statistics		
	Winter	Summer
Mean	1.050	1.057
Std Dev	0.0938	0.0837
Min	0.8100	0.8993
Max	1.1962	1.2296

Source: Own elaboration

The previous statistical results show that the average solar fraction obtained for the winter and summer samples meets the thermal requirements of the industrial process within the range of the independent operating variables.

To carry out the regression with an ANN (artificial neural network), 70% of each sample was used for training, and the remaining 30% was equally divided for validation and testing.

The ANNs constructed for the regression required 15 perceptrons in the hidden layer.

Table 4 presents the most important statistics of the ANN regression.

Box 7

Table 4

ANN regression statistics

	Winter		Summer	
	sf	A	sf	A
MSE	2.7e <sup>-4</sup>	3.5e <sup>-3</sup>	2.7e <sup>-5</sup>	4.7e <sup>-4</sup>
RMSE	1.7e <sup>-2</sup>	5.9e <sup>-2</sup>	5.2e <sup>-3</sup>	2.2e <sup>-2</sup>
R <sup>2</sup>	1.00	0.99	1.00	0.99

Source: Own elaboration

Figure 4 graphically shows the fit of the ANN regression for the solar fraction for the winter and summer seasons concerning the area and the thermal load required by the process.

Box 8

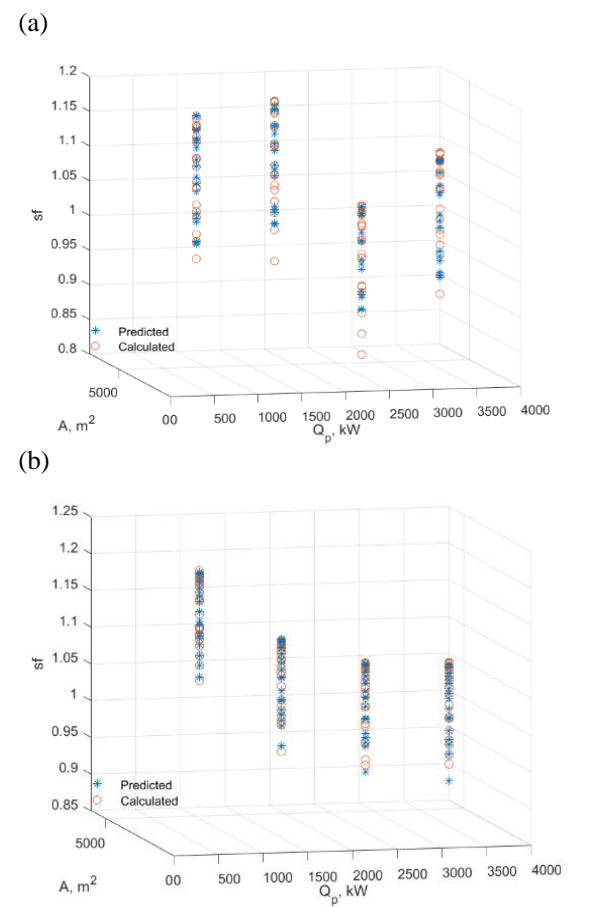
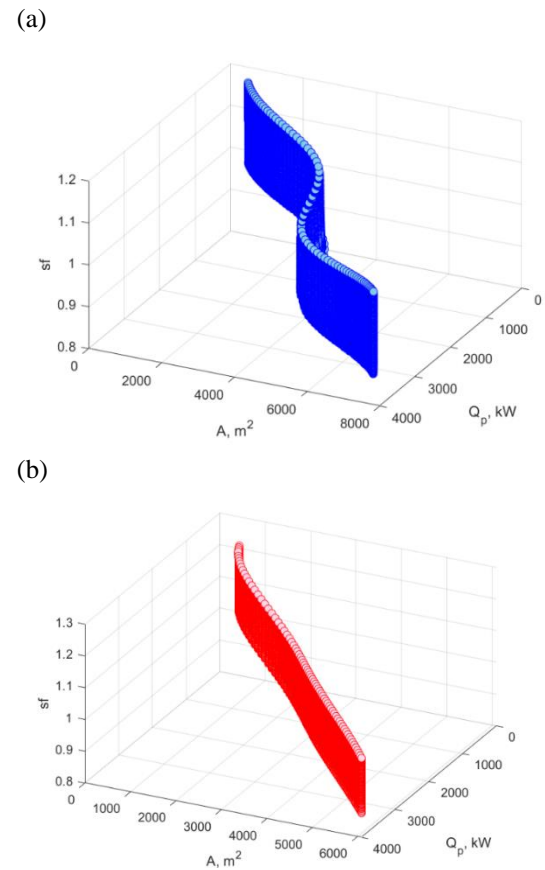


Figure 4  
Fitness of the sf-A regression model: (a) winter and (b) summer  
Source: Own elaboration

Figure 5 presents the profile of the solar fraction estimated through the ANN regression.

Box 9



**Figure 5**  
sf - A performance profile: (a) winter, and (b) summer  
*Source: Own elaboration*

Conclusions

From the previous research, the following conclusions can be drawn:

The proposed optimization process ensures flexible solar thermal networks capable of operating over wide ranges of inlet temperature, process load, and process temperature, generating average solar fractions of 1 for the extreme winter and summer seasons. This allows the thermal requirements of the industrial process to be met throughout the year.

The ANN regression model successfully predicts the behaviour of the variables (sf) and (A) of the solar thermal network for both seasons.

The solar fraction decreases with respect to the required thermal load and the area of the solar thermal network. This effect is more pronounced in the winter season.

Declarations

Conflict of interest

The authors declare no interest conflict. They have no known competing financial interests or personal relationships that could have appeared to influence the article reported in this article.

Authors' Contribution

*Lizárraga-Morazán, Juan-Ramón:* Contributed to the research methodology and generation of results and writing of the manuscript.

*Picón-Núñez, Martín:* Contributed to the project idea, research method, editing and revising of the manuscript.

Funding

No funding was received for the development of this research.

Acknowledgements

CONAHCYT is greatly acknowledged for the postdoctoral grant awarded to Dr. Juan-Ramón Lizárraga-Morazán.

Abbreviations

ANN	Artificial neural network
FFNN	Feed forward neural network
HTF	Heat transfer fluid
MLP	Multilayer perceptron
PVLCE	Present value of life cycle analysis
SHIP	Solar heat for industrial processes

Nomenclature

$A$	Network area, [m²]
$D_i$	Receiver inner diameter, [m]
$Dg_i$	Glass envelope inner diameter, [m]
$f$	Focal distance, [m]
$L$	Row length, [m]
$L_c$	PTC length, [m]
$\dot{m}_f$	Mass flow rate, [kg/s]
$sf$	Solar fraction
$N_{cl}$	Number of collectors per row, [coll/row]
$N_L$	Number of network rows
$Q_p$	Process heat, [kW]
$Q$	Useful heat, [kW]

Article

$q_t$	Instantaneous heat, [kW]
$T_{in}$	HTF Inlet temperature, [°C]
$T_{obj}$	HTF target temperature, [°C]
$T_{HTF}^{limit}$	HTF limit outlet temperature, [°C]
$T_o^{max}$	Maximum outlet temperature, [°C]
$t$	Time, [h]
$W_{aper}$	Width aperture of the PTC, [m].

References

Basics

IRENA. (2024). [RENEWABLE CAPACITY STATISTICS 2024](#). Accessed: Jul. 11, 2024.

United Nations. (2024). [United Nations Sustainable Development GOALS](#). Accessed: Jul. 11, 2024. [Online].

UAE Consensus. (2023). [The UAE Consensus and Action Agenda](#), 2023. Accessed: Jul. 11, 2024.

F. Birol. (2023). [World Energy Investment](#). 1–183.

B. Epp and D. Krüger. (2024). [Overview of global solar process heat market and trends](#).  
R. Adib and A. Zervos (2023). [Renewables 2023 global status report 2023](#).

AEE INTEC (2024). [Solar heat for industrial processes \(SHIP\) plants database](#). Accessed: Feb. 10, 2024. [Online].

S. Kalogirou. (2019). [Solar energy engineering](#). [electronic resource]: processes and systems. Accessed: Jul. 05, 2023. [Online]

Mueller., T. (2004). [PROMISE. Produzieren Mit Sonnenenergie - potential study on thermal solar energy use by the Austrian industry; PROMISE. Produzieren mit Sonnenenergie Potenzialstudie zur thermischen Solarenergienutzung in Oesterreichs Gewerbe- und Industriebetrieben](#). in *14. OTTI symposium on thermal solar energy, 14. OTTI Symposium Thermische Solarenergie*, Ostbayerisches Technologie-Transfer-Institut e.V. (OTTI) and Regensburg (Germany), Eds., Bad Staffelstein (Germany).

Vannoni, C., Drigo, S., Battisti, R., and Schweiger H. (2006). [Ship Plant Survey Report: Solar Heat for Industrial Processes](#): IEA Task 33/IV Subtask A.

Van de Pol, V., and Wattimena, L. (2001). [Onderzoek naar het potentieel van zonthermische energie in de industrie](#), KWA Bedrijfsadviseurs BV, documentn. 8543.00.

Lauterbach, C., Schmitt, B., Jordan, U., and Vajen, K. (2012). [The potential of solar heat for industrial processes in Germany](#). *Renewable and Sustainable Energy Reviews*, vol.16(7),5121–5130.

Differences

González-García, A. (2018). [Potencial de Aplicación de la Energía Solar en Procesos Industriales Térmicos en Chile](#). *Tecnologías Solares para Suministro de Calor en Procesos Industriales*, Santiago de Chile.

Jia, T., Huang, J., Li, R., He, P., & Dai., Y. (2018). [Status and prospect of solar heat for industrial processes in China](#). *Elsevier Ltd*.

Schweiger, H., Farinha, J., & Benz, N. (2000). [The Potential of Solar Heat in Industrial Processes. A State of the Art Review for Spain and Portugal](#).

Aste, N., Del Pero, C., & Leonforte, F. (2012). [Optimization of solar thermal fraction in PVT systems](#). *Energy Procedia*.

Reiter, P., Poier, H., & Holter, C. (2016). [BIG Solar Graz: Solar District Heating in Graz - 500,000 m<sup>2</sup> for 20% Solar Fraction](#). *Energy Procedia*.

F. Pag, F., Jesper, M., Kusyy, O., Vajen, K., & Jordan, U. (2022). [Solar fractions of SHIP plants considering the availability of roof area based on OpenStreetMap data](#). *Solar Energy Advances*, 2.

Lizárraga-Morazan, J.R., and Picón-Núñez, M. (2024). [Harnessing solar power in industry: Heuristic optimisation design and transient thermal modelling of parabolic trough solar collector networks](#). *Chemical Engineering and Processing - Process Intensification*. 200, 109776.

Caballero-Esparza, M., Lizárraga-Morazán, J.R., and Picón-Núñez, M. (2022). [Economic analysis for the selection of low temperature solar thermal utility systems](#). *Appl Therm Eng*, 215,118913.



Sharma, N., Varun, and Siddhartha. (2012). [Stochastic techniques used for optimization in solar systems: A review](#). *Renewable and Sustainable Energy Reviews*, 16(3), 1399–1411.

Afzal, Asif & Buradi, Abdulrajak & Jilte, Ravindra & Shaik, Saboor & Kaladgi, Abdul Razak & Arıcı, Muslum & Lee, Chew Tin & Nižetić, S. (2023). [Optimizing the thermal performance of solar energy devices using meta-heuristic algorithms: A critical review](#). *Renewable and Sustainable Energy Reviews*, 173,112903.

Meyers, R.A. (2013). [Encyclopedia of Sustainability Science and Technology](#). Springer, 7619–7622, 2013. doi: 10.1007/978-1-4419-0851-3.